Charge Transfer in Polypeptides: Effect of Secondary Structures on Charge-Transfer Integral and Site Energies

N. Santhanamoorthi,[†] P. Kolandaivel,*[,†] and K. Senthilkumar[‡]

Department of Physics, Bharathiar University, Coimbatore, India-641 046, and Centre for Computational Chemistry, School of Chemistry, Bristol University, Cantocks Close, Bristol BS8 1TS, United Kingdom

Received: May 18, 2006; In Final Form: July 3, 2006

We have theoretically studied the charge transfer in glycine polypeptide using quantum mechanical models based on a tight-binding Hamiltonian approach. The charge-transfer integrals and site energies involved in the transport of positive charge through the peptide bond in glycine polypeptide have been calculated. The charge-transfer integrals and site energies have been calculated directly from the matrix elements of the Kohn−Sham Hamiltonian defined in terms of the molecular orbitals of the individual fragments of the glycine polypeptide. In addition to this, we have calculated the rate of charge transfer between a neighboring amino acid subgroup through the Marcus rate equation. These calculations have been performed for the different secondary structures of the glycine model peptide such as linear, α-helix, 3_{10}-helix, and antiparallel β-sheet by varying the dihedral angles ω, φ, and ψ along the C_α-carbon of amino acid subgroup. Present theoretical results confirm that the charge transfer through the peptide bond is strongly affected by the conformations of the oligopeptide.

I. Introduction

Charge transport in polypeptide attracts a great deal of interest because of its relevance to biochemical reactions and possible application in molecular electronics.[1,2] The migration of positive charge carriers in polypeptides have been studied extensively. Schlag and co-workers have studied the charge-transfer processes along polypeptides in the gas phase and in hydrated medium employing femtosecond measurements and theoretical methods.[2−8] They observed that the charge transfer through their model peptides is highly efficient for some choices of amino acid subgroups.[4−8] Gray et al. have studied the charge transport in a real protein especially in α-helix (myoglobin) and β-sheet (azurine).[9,10] A few other studies based on ab initio and molecular dynamics calculations have also revealed a long distance charge transport in oligopeptides.[11−15] Migration of charge along the polypeptide chain is due to a hopping mechanism between neighboring amino acid subgroups and is purely electronic property. Only very few theoretical studies have been reported for the charge transport in polypeptides based on molecular orbitals.[1,16]

Charge transport in the polypeptide chain strongly depends on the rotational motion around the bonds along the C_α-carbon of an amino acid subgroup. It was observed that the charge introduced in the polypeptide chain can stay within the subgroup, until the rotational angle reaches to a certain angle at which the charge is transferred to the next subgroup.[3,8] The charge-transfer integral (also called electronic coupling or the hopping matrix element) between the orbitals of amino acid subgroups involved in the charge transport and site energy (energy of the charge when it is localized at a particular amino acid subgroup) are the two important factors that determine the above said critical point and the efficiency of charge transport in a polypeptide chain. The rotational motion in the polypeptide chain is characterized in terms of the set of dihedral angles through the Ramachandran plot,[17] and it determines the dynamics of the charge transport process. Previous studies on charge transport in DNA and discotic liquid crystal molecules show that the charge-transfer integral and site energy are strongly dependent on the structural degrees of freedom.[18,19]

In the longer oligopeptides, the charge transport can be influenced by the secondary structures. In the present investigation, hole transport through a peptide bond has been studied for four secondary structures of oligopeptide based on the energy of molecular orbitals. The requirement for theoretical charge transport models based on molecular orbitals is the charge-transfer integral and site energy. As a reasonable approximation, the positive charge will migrate through the highest occupied molecular orbital (HOMO) of the amino acid subgroups; the charge-transfer integral and site energy corresponding to the HOMO are the two key quantities that need to be calculated. While calculating the charge-transfer integral between the amino acid subgroups in metalloproteins through the energy difference between HOMO and HOMO-1, Prytkova et al.[16] have applied an electric field to bring the site energies of the amino acid subgroups to be identical, which is a common technique in electronic coupling calculation based on the orbital energy splitting method.[1,20,21] In the present study, a method proposed by Siebbeles and co-workers[18,22] based on the fragment orbital approach has been used to calculate the charge-transfer integral and site energy. In this method, the site energy and charge-transfer integral are calculated directly as the diagonal and off-diagonal elements of the Kohn−Sham Hamiltonian. This method is quite suitable to the present work since the site energies of each amino acid subgroup in an oligopeptide are not identical and the overlap between them is not equal to zero.

The charge-transfer integral and site energy are used to estimate the rate of charge transport through peptide bonds in

* To whom correspondence should be addressed. Fax: +91-422-2422387. E-mail: ponkvel@hotmail.com.
[†] Bharathiar University.
[‡] Bristol University.

10.1021/jp063069n CCC: $33.50
Published on Web 09/19/2006

SCHEME 1: Fragment Representation of the Glycine Model Peptide

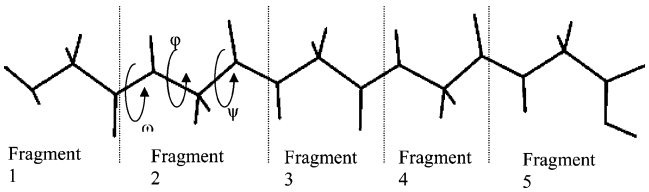

TABLE 1: Dihedral Angles (ω, φ, and ψ, in degrees) Corresponding to a Specific Secondary Structure of Polypeptide[27]

structures	ω	φ	ψ
linear	180	180	180
α-helix	180	−54	−45
3_{10}-helix	180	−60	−30
antiparallel β-sheet	−178	−150	15

four different structures (linear, α-helix, 3_{10}-helix, and antiparallel β-sheet) of oligopeptide through Marcus formula.[23−25] A model peptide consisting of five glycine amino acid subgroups has been taken as the test case. A short theoretical methodology is given in section II. The results of the geometry optimization and stability of secondary structures are discussed in the section IIIa. Calculated charge transport parameters and the rate of charge migration in different secondary structures of oligopeptide are provided and discussed in section IIIb. The conclusions are given in section IV.

II. Theoretical Methodology

The geometry of linear, α-helix, 3_{10}-helix, and antiparallel β-sheet structures of oligopeptide consisting of five glycine amide subgroups have been optimized at the B3LYP/6-311G(d,p) level of theory using the Gaussian 98W program.[26] To retain the geometry of a particular secondary structure, we have performed the constrained optimization by fixing certain dihedral angle values in all the subgroups. Commonly, the secondary structures were defined according to the dihedral angle around the α carbon (C_α) of the amino acid subgroup; the dihedral angles ($C_\alpha CNC_\alpha$), ($CNC_\alpha C$), and ($NC_\alpha CN$) are denoted as ω, φ, and ψ, respectively (see Scheme 1). The average dihedral angle values, ω, φ, and ψ corresponding to a particular secondary structure have been taken from ref 27 and are summarized in Table 1. To ensure the optimized structure corresponds to a global minimum, frequency calculations have been performed.

The presence of excess positive charge in an oligopeptide consisting of n number of amino acid subgroups can be represented in terms of the tight-binding Hamiltonian[28]

$$\hat{H} = \sum_{i=1}^{n} \epsilon_i(\theta) a_i^+ a_i + \sum_{\substack{i,j \\ i \neq j}}^{n} J_{ij}(\theta) a_i^+ a_j \qquad (1)$$

where ϵ_i is the energy of a charge when it is localized at an amino acid subgroup i, called site energy, and J_{ij} represents the charge-transfer integral between the HOMO of subgroups i and j. Both ϵ_i and J_{ij} depend on inter- and intramolecular degrees of freedom, collectively denoted as θ. In eq 1, a_i^+ and a_i are the creation and annihilation operators of a charge on the amino acid subgroup i in the oligopeptide. The site energy, charge-transfer integral, and spatial overlap integral were computed for all the secondary structures using the fragment orbital approach as implemented in the Amsterdam density functional (ADF) theory program.[29]

The model oligopeptide which consisted of five glycine amide subgroups has been represented in terms of five fragments, as shown in Scheme 1. The molecular orbitals generated through single point energy calculation for each fragment have been used as a basis set in further single point energy calculation for full oligopeptide. That is, the molecular orbitals of an oligopeptide are expressed as a linear combination of the molecular orbitals of the individual glycine amide subgroup, φ_i. The output of the final calculation will provide the overlap matrix, **S**, the eigenvector matrix, **C**, and the eigenvalue, **E**. Then the site energy, $\langle\varphi_i|h_{KS}|\varphi_i\rangle$, and charge-transfer integral, $\langle\varphi_i|h_{KS}|\varphi_j\rangle$, are calculated using the relation $\mathbf{h_{KS}} = \mathbf{SCEC}^{-1}$. As described in past studies, this procedure provides a direct and exact calculation for the charge-transfer integral and site energies without invoking the assumption of zero spatial overlap, and it is not necessary to apply an external electric field to bring the site energies of adjacent amino acid subgroups into resonance.[18,21]

The rate for charge transfer through the peptide bond has been calculated according to the Marcus equation[23−25]

$$\upsilon = \frac{J_{\text{eff}}^{\,2}}{\hbar} \sqrt{\frac{\pi}{\lambda k_B T}}\, e^{-(\lambda/4k_B T)} \qquad (2)$$

where J_{eff} is the effective charge-transfer integral, λ is the reorganization energy, and k_B is Boltzmann's constant. The generalized or effective charge-transfer integral, J_{eff}, is used in charge transport calculations, in which the spatial overlap integral is no longer explicitly taken into account, and is equivalent to the charge-transfer integral calculated through orbital energy splitting techniques.[18,21] The effective charge-transfer integral can be defined in terms of charge-transfer integral (J), spatial overlap integral (S), and site energy (ϵ) as[18,21]

$$J_{\text{eff}} = J - \frac{S(\epsilon_1 + \epsilon_2)}{2} \qquad (3)$$

The reorganization energy (λ) of a glycine amide subgroup was calculated through its total energies in neutral and cationic form[30]

$$\lambda = [E^+(g^o) - E^+(g^+)] + [E^o(g^+) - E^o(g^o)] \qquad (4)$$

In eq 4, $E^+(g^o)$ is the total energy of a polypeptide subgroup with an excess positive charge in the optimized neutral geometry, $E^+(g^+)$ is the total energy in optimized cation geometry, and so forth. For open-shell systems, restricted density functional theory (DFT) calculations have been performed.

The use of DFT methods to calculate the parameters related with orbital energies has been discussed extensively.[31,32] In the present work, ADF calculations have been performed with two different exchange correlation potential functionals. In the generalized gradient approximation (GGA) type, Becke's exchange functional[33] is used together with the correlation part of Perdew,[34] denoted as BP. This proceeds from the local density approximation (LDA) for the exchange and correlation functional based on the parametrization of the electron gas data given by Vosko, Wilk, and Nusair (VWN).[35] In addition to this, the DFT calculations have also been performed with the asymptotically corrected exchange correlation potential, SAOP (statistical average of orbital potentials).[32] It has been shown that the HOMO energy calculated through the SAOP potential is in agreement with the vertical ionization energy for various types of molecules,[32] and studies on charge transport in DNA show

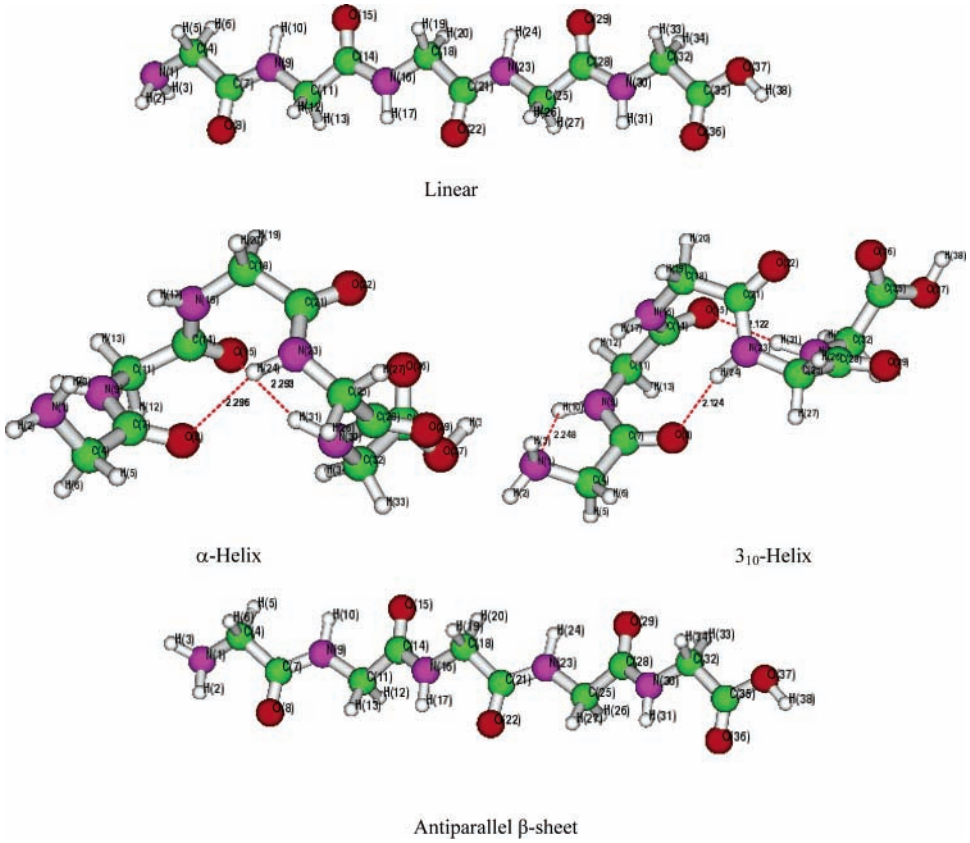

Figure 1. Optimized secondary structures of the glycine model peptide.

that the performance of SAOP is sufficiently good.[19,36] Initial fragment calculations were performed with the atomic basis set consisting of Slater-type orbitals (STOs) of triple-ξ quality including one set of polarization functions on each atom (TZP basis set in ADF).[37]

III. Results and Discussion

IIIa. Structure and Stability of Oligopeptide Conformers. The optimized geometries of oligopeptides are shown in Figure 1. The bond length values of the glycine polypeptide were slightly affected by the rotation of the dihedral angle values (ω, φ, and ψ). It is clear that the linear structure and the antiparallel β-sheet structures have similar bond length values. While comparing the fully extended and helical structures, it has been observed that all the C−N and C−C bond lengths in the helical structures are found to be elongated by 0.01 Å, whereas all the C═O bond lengths are found to be shortened by 0.01 Å.

Further, in the α-helix and 3$_{10}$-helical structures, O···H−N and N···H−N type hydrogen bonds have been noticed. These hydrogen bonds are represented in dotted lines in the Figure 1. Two hydrogen bonds O8···H24−N23 and O15···H31−N30 are formed in the α-helix structure with an O···H distance of 2.296 and 2.293 Å, respectively. Three hydrogen bonds N1···H10−N9, O8···H24−N23, and O15···H31−N30 have been formed in the twisted structure of the 3$_{10}$-helix with the O···H bond length as 2.248, 2.124, and 2.122 Å, respectively. Among the hydrogen bonds which are noticed in the present study, the O15···H31−N30 and O8···H24−N23 hydrogen bonds of the 3$_{10}$-helix structure are the strongest (2.1 Å). Apart from the above-mentioned hydrogen bonds, a number of weak interactions (approaching the van der Waals cutoff limit) were observed in the helical conformers. These weak interactions can contribute to the stabilization of the structure as observed by the earlier studies on the α-helix.[38−40] Further, we have also confirmed the existence of hydrogen bonds in α and 3$_{10}$-helical structures through the values of the Laplacian of electron density, which has been calculated by the MORPHY98[41] program.

TABLE 2: Calculated Relative Energy, ΔE (in kcal/mol), and Dipole Moment, μ_M (in Debye), for the Different Structures of the Glycine Model Peptide

structures	ΔE	μ_M
linear	0.0	9.89
α-helix	10.23	13.29
3$_{10}$-helix	3.39	13.62
antiparallel β-sheet	3.45	8.18

The relative energies of the four conformers of the glycine polypeptide are summarized in Table 2. By comparing the energy values of these secondary structures, it was found that the linear structure is more stable by 10.2 kcal/mol with respect to the least stable α-helix structure. The order of stability is as follows: linear > 3$_{10}$-helix > antiparallel β-sheet > α-helix. The predicted low relative stability of the α-helix structure is rather unexpected since the α-helix structure appears most frequently in proteins and was shown to be favored in a polyglycine model.[39] The recent studies suggest that DFT calculations would underestimate the stability of the α-helix with respect to the 3$_{10}$-helix.[42−44] The dipole moments calculated for helical structures (∼13 D) are much higher than the values calculated for linear and antiparallel β-sheet structures (see Table 2), which conforms the possible higher stabilization of helical structures in solvent medium. Moreover, the oligopeptide structures are stabilized by nonbonded interactions such as hydrogen bonding and intermolecular interactions, which are not completely present in the model peptide considered here.

IIIb. Charge Transport Calculations. In this section, attention has been paid to study the hole transfer between the

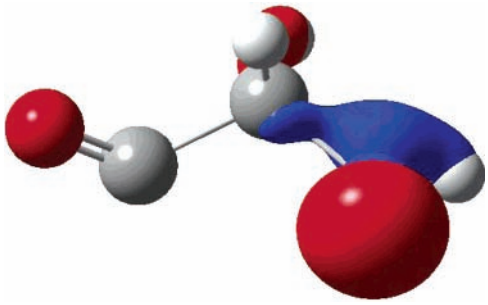

Figure 2. Schematic representation of the highest occupied molecular orbital of the intermediate fragment ($NHCH_2CO$).

TABLE 3: Effective Charge-Transfer Integral (in eV) for Hole Transport between the Fragments 2 and 3 ($J_{eff}1$), 3 and 4 ($J_{eff}2$), and 2 and 4 ($J_{eff}3$) of Different Secondary Structures of the Glycine Model Peptide with SAOP and BP Functionals[a]

	SAOP			BP		
structures	$J_{eff}1$	$J_{eff}2$	$J_{eff}3$	$J_{eff}1$	$J_{eff}2$	$J_{eff}3$
linear	−0.53	−0.52	−0.02	−0.53	−0.52	−0.02
α-helix	−0.51	0.42	−0.07	0.48	0.41	0.07
3_{10}-helix	−0.50	−0.29	0.07	−0.48	0.27	−0.07
antiparallel β-sheet	0.56	0.55	0.01	−0.53	−0.52	−0.02

[a] See Scheme 1 for fragment representation of the model peptide.

fragments 2, 3, and 4 through the peptide bond (C−N) in a model oligopeptide system which consists of five glycine amide subgroups (Scheme 1). We used the SAOP and BP potential functionals in combination with the TZP basis set for the calculation of the charge-transfer integrals and site energies. Since ω, φ, and ψ dihedral angles control the orientation between two adjacent peptide residues in different secondary structures, it can influence the charge-transfer integral between the neighboring amino acid subgroups and their site energy values.

The schematic representation of the HOMO of the amino acid subgroup ($NHCH_2CO$) is shown in Figure 2. The HOMO is delocalized on the region nearer to the nitrogen atom of the amino group (i.e., N-terminus). Similar results have been observed in ADF single point energy calculations for individual fragments. The HOMO of the fragments consists of more than 75% of the nitrogen atom of the amino group. From this, we can expect, in polypeptide, if nitrogen atoms of neighboring amino acid subgroups are nearer then the hole, transport is most favorable.

The calculated charge-transfer integrals and spatial overlap integrals for hole transport between the fragments of glycine model peptide secondary structures are provided in Tables 1S and 2S as Supporting Information. The effective charge-transfer integrals calculated for hole transport between the fragments 2 and 3, 3 and 4, and 2 and 4 are summarized in Table 3, From the tabulated values, it is clear that the charge-transfer integrals calculated using BP and SAOP functionals are almost similar for all the structures. The effective charge-transfer integrals for the hole transport between the fragments 2 and 3 ($J_{eff}1$) and 3 and 4 ($J_{eff}2$) have been found to be maximum values (0.56 and 0.55 eV) in the antiparallel β-sheet structure. The minimum value of the charge-transfer integral, 0.26 eV, is calculated between fragments 3 and 4 ($J_{eff}2$) of the 3_{10}-helix structure.

The value of the effective charge-transfer integral for the hole transport between fragments 2 and 4 ($J_{eff}3$) is found to be maximum (0.07 eV) in the α and 3_{10}-helix structures and it is minimum (0.02 eV) in the linear and antiparallel β-sheet structures. When these three effective charge-transfer integrals are compared, it has been found that the value of the $J_{eff}3$ calculated for extended structures is less. This can explained on the basis of distance between the fragments; the distance between fragment 2 and fragment 4 is found to be 4.6 Å in α and 3_{10}-helix structures, whereas in linear and antiparallel β-sheet structures the fragments are separated by 7.2 Å. The charge-transfer integral values presented in this work are significantly higher than the values of Baranov et al.[45] They have estimated the coupling values between the adjacent amino acid subgroups of the order of 0.1 eV in the model peptide. The smaller value of charge-transfer integral presented in the above work may be due to neglect of spatial overlap and lower level of theory used in the calculation.

TABLE 4: Energy of a Positive Charge When It Is Localized at Fragments 2 (ϵ_1), 3 (ϵ_2), and 4 (ϵ_3) of Glycine Model Peptide Secondary Structures Calculated with SAOP and BP functionals[a]

	SAOP			BP		
structures	ϵ_1	ϵ_2	ϵ_3	ϵ_1	ϵ_2	ϵ_3
linear	−18.571	−18.040	−18.321	−13.408	−13.946	−14.273
α-helix	−18.142	−18.040	−16.121	−14.249	−14.139	−12.155
3_{10}-helix	−18.085	−18.100	−16.584	−14.203	−14.210	−12.646
antiparallel β-sheet	−17.582	−17.939	−18.195	−13.586	−13.972	−14.289

[a] See Scheme 1 for fragment representation of the model peptide.

The site energies which are calculated as the diagonal matrix elements of the Kohn−Sham Hamiltonian are given in Table 4 for the different structures of the glycine model polypeptide. Here, ϵ_1, ϵ_2, and ϵ_3 represent the site energies of the fragments 2, 3, and 4, respectively. The calculated site energy values using SAOP and BP functional gave similar results. The comparison of the HOMO energies of individual amino acid subgroups (fragments 2, 3, and 4) and the site energies for the hole transport in the model peptide indicates that the site energy values (ϵ_1, ϵ_2, and ϵ_3) are found to be decreased by approximately 5 eV for all the secondary structures. The HOMO energy calculated for an individual fragment at the BP/TZP level of theory is approximately 7 eV, and at the SAOP/TZP level of theory, the HOMO energy is approximately 12 eV. The rotation of dihedral angles changes the site energy value maximum 0.5 eV. This difference in site energy value may lead to a considerable barrier for charge transport between neighboring amino acid subgroups at a particular conformation.

The reorganization energy (λ) due to the presence of positive charge has been calculated for the model peptide subgroup by using eq 4. The additional hydrogen atoms were added at the N and C termini to satisfy the valences. The reorganization energy is found to be 1.03 eV for the presence of the hole. By analyzing the optimized geometries of the neutral and cation species, it has been found that the presence of excess positive charge changes the bond lengths and bond angles significantly. The bond length C−C has been observed to be increased by 0.2 Å, whereas the bond length N−H is found to be decreased by 0.1 Å in the cation compared with the neutral species. The calculated effective charge-transfer integral with the BP functional combined with the reorganization energy have been used to calculate the rate of charge transport (υ) between neighboring fragments using eq 2. The calculated rate of charge transport between fragments 2 and 3, and 3 and 4 is plotted with respect to the different structures of the glycine model peptide and is shown in Figure 3. The maximum hole transport rate between fragments has been calculated in the antiparallel β-sheet and linear structures (1.33×10^{11} S^{-1}). The minimum rate of 3.47×10^{10} S^{-1} has been calculated between fragments 3 and 4 in

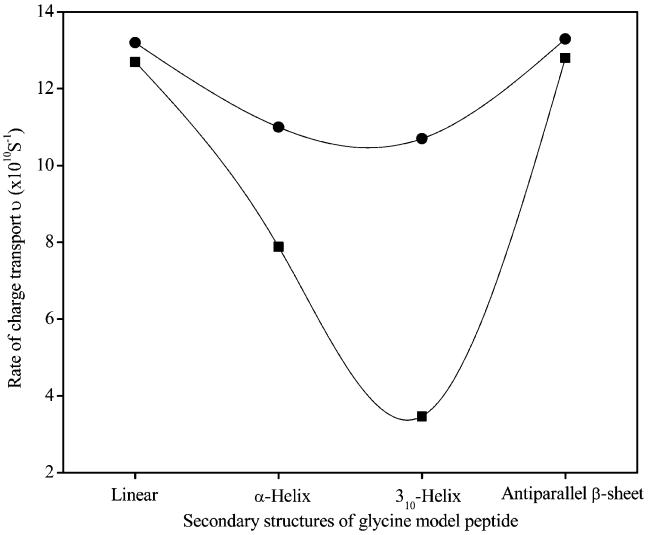

Figure 3. Rate of hole transport between the fragments 2 and 3 (circle) and 3 and 4 (square) of glycine model peptide secondary structures.

the 3_{10}-helix. The rotation of the dihedral angle along the C_α-carbon of fragments 3 and 4 in the 3_{10}-helix (C18C21N23H24) changes the orientation of the C−N bonds by 11° compared with linear or antiparallel β-sheet structures. This reduces the charge-transfer integral and rate of charge transport between them by a factor of 2. The above results show that the rate of charge transport across the oligopeptide is strongly influenced by the secondary structure and dynamics of the dihedral angle. Hence, to obtain the qualitative rate of charge transport in oligopeptide, one needs information about the dynamics of the dihedral angle along the C_α-carbon of the amino acid subgroup.

IV. Conclusions

The charge-transfer integrals and site energies for hole transport through the peptide bond in a model oligopeptide consisting of five glycine amino acid subgroups have been calculated. These parameters were calculated for four different secondary structures (linear, α-helix, 3_{10}-helix, and antiparallel β-sheet) of model peptide. The geometry of the secondary structures was optimized at the B3LYP/6-311G(d,p) level of theory. The rotation of the dihedral angles ω, φ, and ψ of the amino acid subgroups significantly affects the main chain bond lengths. The optimized structures differ considerably in energy, and the order of stability of the structures is linear > 3_{10}-helix > antiparallel β-sheet > α-helix.

The charge-transfer integrals and site energies were obtained directly as the matrix elements of the Kohn−Sham Hamiltonian using the fragment orbital approach as implemented in the ADF program. The rotation of the dihedral angles (ω, φ, and ψ) in the model peptide significantly influences the charge-transfer integrals. The site energy values calculated for the amino acid subgroups reveal a maximum barrier of 0.5 eV at certain dihedral angle values. The rate of charge transport between the neighboring amino acid subgroups has been calculated by using the Marcus rate equation, and the results confirm that the structural changes in the form of dihedral angle changes along the C_α-carbon of each amino acid subgroup strongly affects the rate of charge transport in oligopeptides.

Acknowledgment. The authors are thankful to the DST (Department of Science and Technology), Government of India for establishing the Central Computer Lab under the DST-FIST program, where most of the calculations have been performed.

Supporting Information Available: The calculated charge-transfer integral and spatial overlap integral for the charge transport between fragments are given in Tables 1S and 2S. The site energies of the first and last fragments of glycine model peptide secondary structures are given in Table 3S. This material is available free of charge via the Internet at http://pubs.acs.org.

References and Notes

(1) Gray, H. B.; Winkler, J. R. *Q. Rev. Biophys.* **2003**, *36*, 341.
(2) Sheu, S.-Y.; Yang, D.-Y.; Selzle, H. L.; Schlag, E. W. *Eur. Phys. J. D* **2002**, *20*, 557.
(3) Schlag, E. W.; Sheu, S.-Y.; Yang, D.-Y.; Selzle, H. L.; Lin, S. H. *J. Phys. Chem. B* **2000**, *104*, 7790.
(4) Sheu, S.-Y.; Yang, D.-Y.; Selzle, H. L.; Schlag, E. W. *J. Phys. Chem. A* **2002**, *106*, 9390.
(5) Lehr, L. *J. Phys. Chem. A* **2005**, *109*, 8074.
(6) Sheu, S.-Y.; Schlag, E. W.; Yang, D.-Y.; Selzle, H. L. *J. Phys. Chem. A* **2001**, *105*, 6353.
(7) Kulhanek, P.; Schlag, E. W.; Koca, J. *J. Am. Chem. Soc.* **2003**, *125*, 13678.
(8) Schlag, E. W.; Sheu, S.-Y.; Yang, D.-Y.; Selzle, H. L.; Lin, S. H. *Proc. Natl. Acad. Sci. U.S.A.* **2000**, *97*, 1068.
(9) Winkler, J. R.; Gray, H. B. *J. Biol. Inorg. Chem.* **1997**, *2*, 399.
(10) Mayo, S. L.; Ellis, W. R. J.; Crutchley, R. J.; Gray, H. B. *Science* **1986**, *233*, 948.
(11) Beratan, D. N.; Onuchic, J. N.; Winkler, J. R.; Gray, H. B. *Science* **1992**, *258*, 1740.
(12) Remacle, F.; Ratner, M. A.; Levine, R. D. *Chem. Phys. Lett.* **1998**, *25*, 285.
(13) Jones, G., II; Lu, L. N.; Fu, H.; Farahat, C. W.; Oh, C.; Greenfield, S. R.; Gosztola, D. J.; Wasielewski, M. R. *J. Phys. Chem. B* **1999**, *103*, 572.
(14) Prutz, W. A.; Land, E. J. *Int. J. Radiat. Biol.* **1979**, *36*, 513.
(15) Improta, R.; Antonello, S.; Formaggio, F.; Maran, F.; Rega, N.; Barone, V. *J. Phys. Chem. B* **2005**, *109*, 1023.
(16) Prytkova, T. R.; Kurnikov, I. V.; Beratan, D. N. *J. Phys. Chem. B* **2005**, *109*, 1618.
(17) Ramachandran, G. N.; Sasisekharan, V. *Adv. Protein Chem.* **1968**, *23*, 283.
(18) Senthilkumar, K.; Grozema, F. C.; Bickelhaupt, F. M.; Siebbeles, L. D. A. *J. Chem. Phys.* **2003**, *119*, 9809.
(19) Senthilkumar, K.; Grozema, F. C.; Guerra, C. F.; Bickelhaupt, F. M.; Lewis, F. D.; Berlin, Y. A.; Ratner, M. A.; Siebbeles, L. D. A. *J. Am. Chem. Soc.* **2005**, *127*, 14894.
(20) Stuchebrukhov, A. A. *Theor. Chem. Acc.* **2003**, *110*, 291.
(21) Newton, M. D. *Chem. Rev.* **1991**, *91*, 767.
(22) van Eijck, L.; Senthilkumar, K.; Siebbeles, L. D. A.; Kearley, G. J. *Physica B* **2004**, *350*, 220.
(23) Marcus, R. A.; Sutin, N. *Biochim. Biophys. Acta Rev. Bioenerg.* **1985**, *811*, 265.
(24) Mikkelsen, K. V.; Ratner, M. A. *Chem. Rev.* **1987**, *87*, 113.
(25) Bixon, M.; Jortner, J. *Chem. Phys.* **2002**, *281*, 393.
(26) Frisch, M. J.; Trucks, G. W.; Schlegel, H. B.; Scuseria, G. E.; Robb, M. A.; Cheeseman, J. R.; Zakrzewski, V. G.; Montgomery, J. A.; Stratmann, R. E.; Burant, J. C.; Dapprich, S.; Millam, J. M.; Daniels, A. D.; Kudin, K. N.; Strain, M. C.; Farkas, O.; Tomasi, J.; Barone, V.; Cossi, M.; Cammi, R.; Mennucci, B.; Pomelli, C.; Adamo, C.; Clifford, S.; Ochterski, J.; Petersson, G. A.; Ayala, P. Y.; Cui, Q.; Morokuma, K.; Malick, D. K.; Rabuck, A. D.; Raghavachari, K.; Foresman, J. B.; Cioslowski, J.; Ortiz, J. V.; Stefanov, B. B.; Liu, G.; Liashenko, A.; Piskorz, P.; Komaromi, I.; Gomperts, R.; Martin, R. L.; Fox, D. J.; Keith, T.; Al-Laham, M. A.; Peng, C. Y.; Nanayakkara, A.; Gonzalez, C.; Challacombe, M.; Gill, P. M. W.; Johnson, B. G.; Chen, W.; Wong, M. W.; Andres, J. L.; Head-Gordon, M.; Replogle, E. S.; Pople, J. A. *Gaussian 98*; Gaussian, Inc.: Pittsburgh, PA, 1998.
(27) Csaszar, A. G.; Perczel, A. *Prog. Biophys. Mol. Biol.* **1999**, *71*, 243.
(28) Silinsh, E. A. *Organic molecular crystals*; Springer-Verlag: Berlin, 1980.
(29) te Velde, G.; Bickelhaupt, F. M.; Baerends, E. J.; Fonseca Guerra, C.; van Gisbergen, S. J. A.; Snijders, J. G.; Ziegler, T. *J. Comput. Chem.* **2001**, *22*, 931.
(30) Tavernier, H. L.; Fayer, M. D. *J. Phys. Chem. B* **2000**, *104*, 11541.
(31) Dreuw, A.; Head-Gordon, M. *J. Am. Chem. Soc.* **2004**, *126*, 4007.
(32) Chong, D. P.; Gritsenko, O. V.; Baerends, E. J. *J. Chem. Phys.* **2002**, *116*, 1760.
(33) Becke, A. D. *Phys. Rev. A* **1988**, *38*, 3098.
(34) Perdew, J. P. *Phys. Rev. B* **1986**, *33*, 8822.
(35) Vosko, S. H.; Wilk, L.; Nusair, M. *Can. J. Phys.* **1980**, *58*, 1200.

(36) Senthilkumar, K.; Grozema, F. C.; Guerra, C. F.; Bickelhaupt, F. M.; Siebbeles, L. D. A. *J. Am. Chem. Soc.* **2003**, *125*, 13658.
(37) Snijders, J. G.; Vernooijs, P.; Baerends, E. J. *At. Data Nucl. Data Tables* **1981**, *26*, 483.
(38) Chothia, C. *Annu. Rev. Biochem.* **1984**, *53*, 537.
(39) Hol, W. G. J.; van Duijnen, P. T.; Berendsen, H. J. C. *Nature* **1978**, *273*, 443.
(40) Hol, W. G. J. *Adv. Biophys.* **1985**, *19*, 133.
(41) *MORPHY98*, a program written by P. L. A. Popelier with a contribution from R. G. A. Bone; UMIST: Manchester, U.K., 1998.
(42) Improta, R.; Barone, V. *J. Chem. Phys.* **2001**, *114*, 2541.
(43) Wu, Q.; Yang, W. *J. Chem. Phys.* **2002**, *116*, 515.
(44) Improta, R.; Barone, V.; Kudin, K.; Scuseria, G. E. *J. Chem. Phys.* **2001**, *114*, 2541.
(45) Baranov, L. Ya; Schlag, E. W. *Z. Naturforsch., A: Phys. Sci.* **1999**, *54*, 387.